Heavy Quark Spectroscopy at LHCb

D. Johnson([1])([*])
on behalf of the LHCb collaboration
([1]) *CERN, CH 1211, Genève 23, Suisse*

Summary. — Great progress has been made in recent years in the study of hadron spectroscopy, particularly in the investigation of particles formed from exotic combinations of quarks. The LHCb experiment is well suited to the study of such particles. In this report, studies by the LHCb collaboration of the $X(3872)$ and $Z(4430)$ resonances, as well as the observation of two pentaquark states, are described.

PACS 29.30.Ep – Charged-particle spectroscopy.
PACS 14.40.Pq – Heavy quarkonia.
PACS 14.40.Rt – Exotic mesons.
PACS 14.20.Pt – Exotic baryons.

1. – Introduction

Since the development of the quark model in the 1960s, hadronic bound states have been thought to be formed either from a quark-antiquark pair (a 'meson' state) or from three quarks or antiquarks (a 'baryon'). The success of this picture is clear, for example, in a consideration of the charmonium spectrum. Given the large mass of the charm quark with respect to the scale of quantum chromodynamics (QCD), $c\bar{c}$ bound states can be described using a simple potential model. The model contains two terms: a Coulomb-like term, corresponding to single gluon exchange, and a linearly increasing term, implementing the 'confinement' of QCD. Below the open charm threshold the observed states are found to correspond closely to those predicted.

Despite long-standing expectations (e.g. [1]) that more complicated combinations of quarks could be made, none had yet been observed conclusively at the turn of the century. However, since the first observation of the $X(3872)$ resonance in 2003 [3] it has become clear that the picture of the charmonium spectrum above the open charm threshold is considerably less clear than that below; only a few of the predicted states have actually been observed, and many of the states that have been cannot be easily associated with any of those predicted. Many models have been proposed to explain this structure.

([*]) daniel.johnson@cern.ch

I begin with a discussion of the features of the LHCb detector that make it particularly useful for studies of hadronic spectroscopy, and follow with a consideration of three recent results of particular interest. First of all, recent progress in understanding what is widely accepted to be the first exotic multi-quark final state, the $X(3872)$, is presented. The second topic is a second minimally four-quark state, the $Z(4430)$, and the recent confirmation of its quantum numbers. Finally I turn to the discovery only last year of the pentaquark, the first in a previously unseen class of particles formed from five quarks.

2. – Spectroscopy at LHCb

The LHCb detector is very well suited to studies of spectroscopy, in particular for those studies that involve muons and/or charged hadrons [2]. Its combination of a multi-layer silicon detector situated 8 mm from the beam, four planes of silicon or straw-tube tracking detectors, and a 4 Tm warm dipole magnet allow impact parameter resolutions of as low as 15 μm to be obtained, as well as a momentum resolution between 0.5 % and 1.0 %. Two Ring Imaging Cherenkov detectors, either side of the dipole magnet, provide discrimination between particle types and are principally used to separate protons, kaons and pions.

The data used in the studies reported were collected in 2011 and 2012 during the LHC Run 1, and during this time the LHCb experiment benefitted from an efficient hadronic trigger. The first-level hardware trigger made heavy use of information from the muon and calorimetry systems, reducing the 20 MHz pp crossing rate to an overall trigger rate of just 1 MHz. Two successive and increasingly sophisticated levels of software trigger followed, exploiting the characteristic decay topology (e.g. displaced vertices) and particle kinematics (e.g. large p_{T}) typically observed in the decays of the heavy quark hadrons that the experiment was designed to study.

Two techniques have been used to great effect in a wide range of analyses of spectroscopy, where the final state involves three particles. The first is the amplitude analysis of the three-body phase space, whose degrees of freedom are often represented by two-dimensional 'Dalitz plots' of the squared invariant masses of pairs of the final state particles. Resonances, exotic or otherwise, appear as dense bands across the Dalitz plot which, in the case of a non-resonant decay, would be uniformly populated. Resonant bands are modulated by a function depending on the spin of the intermediate resonance. The nature of apparent enhancements in the Dalitz plot can be further probed in a quasi model-independent fashion by allowing additional degrees of freedom in amplitude models of the Dalitz plot, corresponding to the complex phase of the new amplitude. By comparing the variation of the phase through the region of the Dalitz plot containing the new resonance with that expected for a standard Breit-Wigner resonance lineshape, the resonant nature of intriguing enhancements can be established with increased confidence. Studies of Dalitz plots and exotic resonance phase variations are central to many of the investigations that are presented here.

3. – The $X(3872)$

The $X(3872)$ resonance was first observed by the Belle collaboration more than a decade ago [3] in a sample of $B^{\pm} \to K^{\pm} J/\psi \pi^+ \pi^-$ decays. It appeared as a very narrow structure in the $J/\psi \pi^+ \pi^-$ spectrum with a mass around 3872 MeV/c^2 and width of order 1 MeV/c^2, and has been studied further using data from no fewer than six further experiments [4, 5, 6, 7, 8, 9]. The energy release involved in the $X(3872)$ decay to

$J/\psi\pi^+\pi^-$ is small, so the $c\bar{c}$ pair must be present in the initial bound state. A simple pure charmonium interpretation of the resonance is disfavoured for a number of reasons, not least of which is the observation of large isospin violation in its decays to $J/\psi\pi^+\pi^-$ and $J/\psi\pi^+\pi^-\pi^0$ [6, 10]. There have been a number of attractive proposals to account for the state including molecular models, prompted by the proximity of the state to the $D^0\bar{D}^{*0}$ threshold [11], tetraquark explanations, though these lead to the expectation for a second state nearby [12], hybrid states involving excitation of the intervening gluon field [13], vector glueballs [14] and admixtures of these [15].

The first determination of the $X(3872)$ quantum numbers came from an angular analysis of 2,300 inclusively reconstructed $X(3872) \to J/\psi\pi^+\pi^-$ decays by the CDF collaboration [16]. This was followed by the LHCb collaboration with a full five dimensional angular analysis of 300 $B^\pm \to K^\pm X(3872)$ candidate decays [17], obtained from data collected only in 2011. This analysis assumed the lowest possible angular momentum for the $J/\psi\pi^+\pi^-$ system, reasonable given the low energy release in the decay, but it is not hard to imagine that an exotic internal $X(3872)$ structure could result in this assumption being challenged. The angular analysis was therefore performed using the full Run 1 LHCb dataset and a sample of around 1,000 $B^\pm \to K^\pm X(3872)$ candidates [18]. A minimum negative log likelihood fit was performed for a range of different J^{PC} hypotheses, up to $J = 4$, allowing for various values of orbital angular momentum and spin by means of varying helicity couplings. The preferred configuration was found to be $J^{PC} = 1^{++}$, and the difference in the negative log likelihood, $t = -2\log\left(\frac{\mathcal{L}_{\text{alternative}}}{\mathcal{L}_{1^{++}}}\right)$, was determined with respect to each alternative hypothesis. Carrying out pseudoexperiments, generated at the best-fit point and where the fit was performed under various J^{PC} hypotheses, allowed the level of discrimination between the different J^{PC} to be quantified. The distributions of t under the 1^{++} and the alternative hypothesis are shown in Fig. 1 in the red (dashed line) and blue (solid line) histograms, respectively, where the black line indicates the difference in t found in the fit to data. All alternative hypotheses tested are excluded at more than sixteen standard deviations. By considering the values obtained for the coefficients of the various helicity couplings, corresponding to $L, S \in [(0,1),(2,1),(2,2)]$, an upper limit is placed on the D-wave fraction of the state at 4% with a 95% confidence level, which suggests that a smaller, more compact, state is preferred for the $X(3872)$.

Another avenue to gain understanding of the nature of the $X(3872)$ is through the study of its radiative transitions, since electromagnetic transitions amongst charmonium states are well defined, and potential models provide precise predictions. Searches for radiative $X(3872)$ decays were successful, and evidence of its decay to $J/\psi\gamma$ appeared as early as 2006, constraining the C-parity of the state to be even [19]. A further insight into the nature of the $X(3872)$ is obtained through the measurement of the ratio of $X(3872)$ branching fractions to $J/\psi\gamma$ and $\psi(2S)\gamma$. Different models yield very different predictions for this ratio, $R_{\psi\gamma}$, with molecular interpretations favouring a value of order 0.003 [20], pure charmonium models yielding values between 1.2 and 15 [21], and admixture models giving values between 0.5 and 5 [22]. Studies by the BaBar collaboration led to a clear signal in the $\psi(2S)\gamma$ channel and a value for $R_{\psi\gamma}$ of 3.4 ± 1.4 [23], but the Belle collaboration did not find a signal. Whilst remaining compatible with the BaBar result, they placed only an upper limit on the ratio: $R_{\psi\gamma} < 1.2$ at the 95 % confidence level [24]. Employing the full Run 1 LHCb dataset, signals of 600 $X(3872) \to J/\psi\gamma$ and 40 $X(3872) \to \psi(2S)\gamma$ decay candidates are seen in Fig. 2, and the ratio $R_{\psi\gamma} = 2.46 \pm 0.64$ (stat.) ± 0.29 (syst.) is measured [25]. The main contributions to the systematic uncertainty arise from uncertainty on the fit functions used to model signal

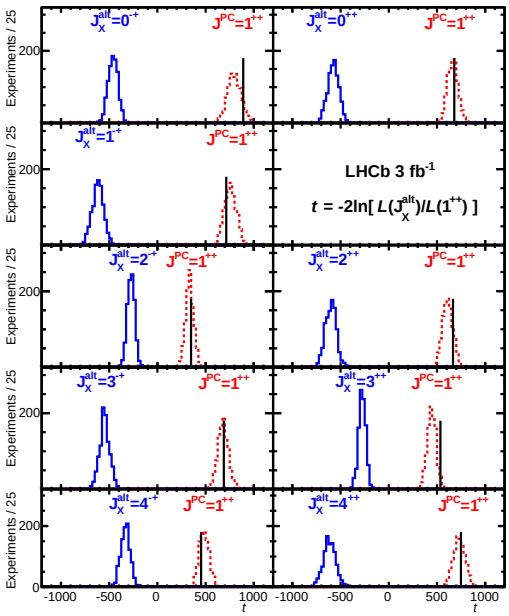

Fig. 1. – Pseudoexperiments are performed by generating according to the best fit result and fitting with a variety of models. The distributions show the difference in the negative log likelihood between fits with alternative J^{PC} hypotheses and the fit with $J^{PC} = 1^{++}$ [18].

and background, and from limited knowledge of the photon reconstruction efficiency. This measurement is compatible with those made by BaBar and Belle, whilst improving significantly on their precision, and contradicts the predictions of the pure molecular models. With the pure molecular hypothesis strongly disfavoured, attention will continue to be focussed on this state in order to establish whether the $X(3872)$ is pure charmonium after all, or perhaps a charmonium-molecule admixture.

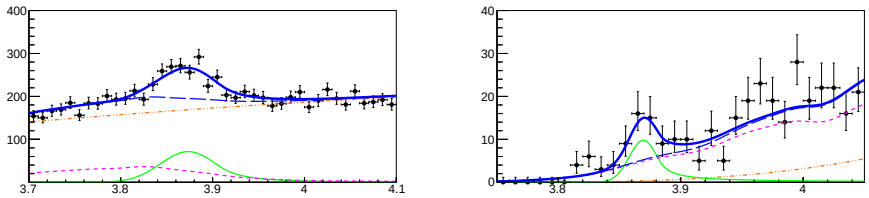

Fig. 2. – Results of an LHCb study of radiative $X(3872)$ decays. The left figure shows the large $X(3872) \to J/\psi\gamma$ signal; the right shows the clear signal of the $X(3872) \to \psi(2S)\gamma$ decay [25].

4. – The $Z(4430)$

The $Z(4430)$ was first observed in 2008 in samples of $B \to K\psi(2S)\pi^{\mp}$ and $B \to KJ/\psi\pi^{\mp}$ decays recorded by the Belle experiment [26]. Appearing as an enhancement in the $\psi^{(\prime)}\pi^{\pm}$ spectrum, with a mass of 4,433 MeV/c^2, the $Z(4430)$ is light enough that

it must contain a $c\bar{c}$ pair. Whilst its narrow width, just $45\,\mathrm{MeV}/c^2$, means that it is unlikely to occur as the result of a reflection from resonances formed in the $K\pi$ system, its confirmation at another experiment is crucial to unambiguously establish its status as the first charged exotic hadron candidate to be discovered. As for the $X(3872)$, a range of theoretical interpretations of the enhancement have been proposed, including S-wave threshold effects, motivated by the nearby $D^*D_1(\bar{2}420)$ threshold [27], standard molecular interpretations [28], and diquark-diantiquark excitations [29].

Employing the full Run 1 dataset, the LHCb collaboration made a study of the $Z(4430)$ [30], benefitting from a sample approximately ten times larger than that used in the original Belle discovery paper. In total a sample of 25,000 $B^0 \to K^{\pm}\psi(2S)\pi^{\mp}$ candidates is prepared, with very high purity, around 97%. Even a visual inspection of the Dalitz plot, shown in Fig. 3, reveals a horizontal band corresponding to an enhancement in the $\psi(2S)\pi^{\mp}$ channel, a little below $m(\psi(2S)\pi^{\mp})^2 = 20\ \mathrm{GeV}^2/c^4$.

In order to study the visible excess further, the shape of the small background contamination is obtained from portions of the high and low B^0 invariant mass spectrum, where combinatorial background dominates. The variation of the various selection efficiencies across the Dalitz plot are obtained using simulated samples. Before carrying out a full amplitude analysis, a model independent approach is taken to test whether the $\psi(2S)\pi^{\mp}$ channel enhancement can be explained solely in terms of reflections of resonances formed between the $K\pi$ pair. The 'ith-order moments', up to fourth order, of the $K\pi$ system are obtained according to a Legendre polynomial of order i in the $K\pi$ helicity angle, and these are reflected into the $\psi(2S)\pi^{\mp}$ channel by weighting a large sample of simulated $B^0 \to K^{\pm}\psi(2S)\pi^{\mp}$ decays. The effect of background in the data set is removed from the sample using a sideband subtraction and, after the remaining candidates are efficiency corrected, comparison can be made with the reflected $K\pi$ moments as shown in Fig. 3. The reflected moments describe the data well except in the region where the $Z(4430)$ resonance is expected to contribute, where the disagreement is pronounced. Clearly reflections of $K^* \to K^{\pm}\pi^{\mp}$ resonances cannot explain the excess at $m(\psi(2S)\pi^{\mp})^2 = 20\ \mathrm{GeV}^2/c^4$.

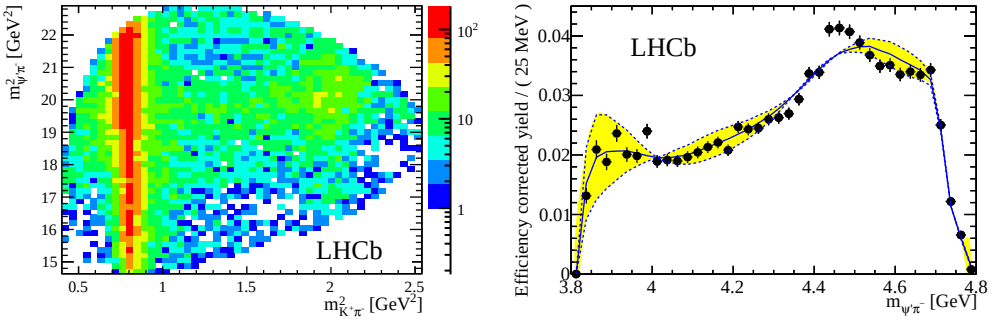

Fig. 3. – Evidence of the exotic $Z(4430)$ resonance [30]. The left figure is the Dalitz plot of the $B^0 \to K^{\pm}\psi(2S)\pi^{\mp}$ candidates, where the horizontal band just below $m(\psi(2S)\pi^{\mp})^2 = 20\ \mathrm{GeV}^2/c^4$ corresponds to the $Z(4430)$. On the right is shown the result of reflecting moments up to order four in the $K\pi$ system to the $\psi(2S)\pi^{\mp}$ channel, where a significant discrepancy between background-subtracted, efficiency-corrected data and reflected moments is apparent exactly where the $Z(4430)$ resonance is expected.

The second approach is the construction of an amplitude model to describe the structure formed in the Dalitz plot by resonances. The isobar formalism is followed, where the overall decay amplitude is formed from the coherent sum of amplitudes corresponding to each resonance that is considered to be formed between pairs of the final state particles, with the lineshape for each often represented by a Breit Wigner [31]. All known neutral K^* resonances falling within, and just outside, the kinematic limits are considered. The masses and widths of each resonance are fixed to their nominal values, except for the $K^*(800)$, $K^*(892)$ and $K_2^*(1430)$ widths and the $K^*(800)$ mass which are allowed to vary. An S-wave nonresonant term is included. The results of the best fit are shown in Fig. 4, where the need for the inclusion of the $Z(4430)$, with $J^P = 1^+$ is clear. The alternative $J^P = 0^-$ hypothesis is examined using the same procedure as for the $X(3872)$, and is excluded at more than 5σ.

A final test of the resonant nature of the $Z(4430)$ is performed by replacing the $Z(4430)$ amplitude with freely varying complex parameters in six regions of $m(\psi(2S)\pi^{\mp})$ invariant mass. The data are fit with this new function, and the six complex parameters are shown on the Argand diagram in Fig. 4. Standard 'phase rotation' is exhibited, and is seen to be compatible with that expected for a Breit Wigner function. The $Z(4430)$ resonance is confirmed using LHCb data, and its quantum numbers established to be $J^P = 1^+$ with high confidence.

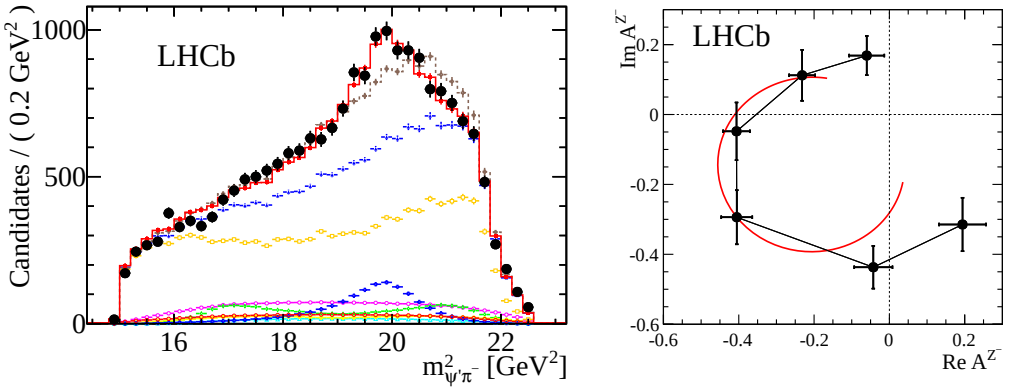

Fig. 4. – Study of the $Z(4430)$ resonance amplitude [30]. The left figure shows the best amplitude model. The data are shown (black points) with the overall model superimposed (red histogram). Components are added according to their fit-fractions: a coherent sum of decay amplitudes corresponding to an S-wave nonresonant term (pink points), a range of neutral K^* resonances (various colours), and the $Z(4430)$ resonance amplitude (dark blue points forming a peaking structure at $m(\psi(2S)\pi^{\mp})^2 = 20$ GeV$^2/c^4$). The right figure shows the Argand diagram obtained when six complex parameters are introduced to account for the excess instead of a Breit Wigner function. The values extracted from the fit are shown (black points) and correspond closely to the pattern expected for a genuine resonance with a Breit Wigner lineshape (smooth red curve).

5. – The $P_c(4380)$ and $P_c(4450)$

The decay process $\Lambda_b^0 \to J/\psi p K^-$ was studied by the LHCb collaboration using data collected during 2011 to measure precisely the Λ_b^0 lifetime [32]. However, during

studies of the full Run 1 dataset, corresponding to 26,000 candidates with 95% purity, a sharp structure became clear in the $J/\psi p$ channel in the region of invariant mass around $4.4\,\mathrm{GeV}/c^2$ [33]. Such a structure is not expected in this channel, in which only reflections from excited $\Lambda \to pK^-$ would be anticipated to produce structure; a resonance decaying to the $J\psi p$ final state must have minimal, exotic, quark content $c\bar{c}uud$. Alternative explanations are excluded: efficiency variations are smooth in the $J/\psi pK^-$ Dalitz plot; peaking backgrounds, such as $B_s^0 \to J/\psi K^+K^-$ and $B^0 \to J/\psi \pi^+K^-$ are specifically vetoed; and only unique tracks of good quality are used to construct the candidates.

In order to verify that the structure cannot be explained simply in terms of Λ^* reflections, a six-dimensional amplitude fit is performed including all known Λ^* states but not accounting for any new contributions in the $J/\psi p$ spectrum. An excellent description of the pK^- invariant mass spectrum is achieved, but the amplitude model fails to account for the structure in the $J/\psi p$ spectrum. Neither allowing masses and widths to vary, nor adding new pK^- resonances and non-resonant contributions, achieves a satisfactory description. However, a good description of the Dalitz plot can be achieved when not one but two new states with opposite parity are introduced in the $J/\psi p$ channel. The first, a lighter but broader state, has a mass of $4.38\,\mathrm{GeV}/c^2$ and a width of $205\,\mathrm{MeV}/c^2$ whilst the second, heavier and narrower, has a mass of $4.45\,\mathrm{GeV}/c^2$ and a width of $40\,\mathrm{MeV}/c^2$. The fit to data including these two new states is visualised in Fig. 5.

The resonant nature of the new states is further probed, using the same technique as was described for the $Z(4430)$ studies, by floating complex parameters in place of the standard Breit Wigner function. The resulting Argand diagrams for the two states are shown in Fig. 6, where the typical resonance phase rotation behaviour is visible for both states, albeit limited by statistical variations. A full determination of the quantum numbers of the states will be possible as the LHCb dataset is augmented.

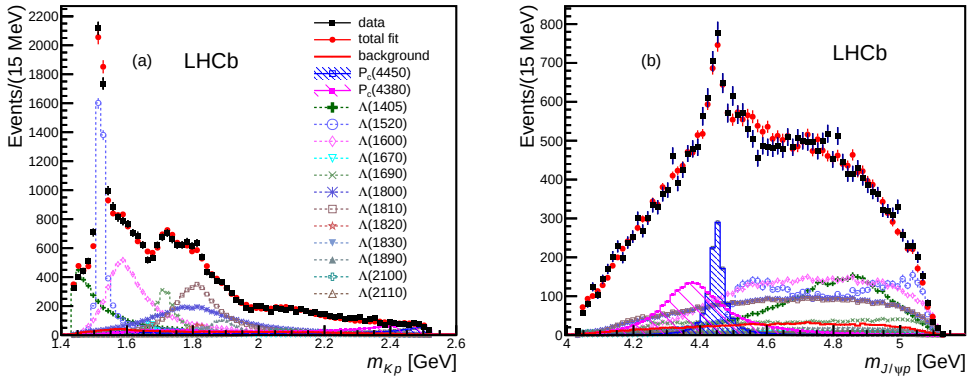

Fig. 5. – Amplitude model fit to the $J/\psi pK^-$ data sample (black points) where the overall fit function is superimposed (red points), as are histograms corresponding to the individual fit components for each resonance included. The pK^- spectrum is shown in the left image, and the $J/\psi p$ spectrum is given on the right. The fit components corresponding to the two new pentaquark states are represented by the shaded histograms [33].

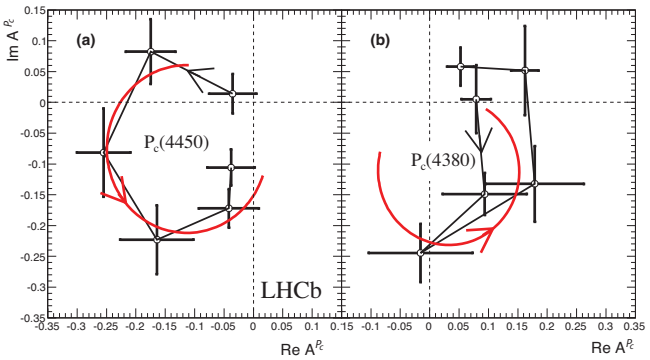

Fig. 6. – Phase rotation of the two new pentaquark states [33].

REFERENCES

[1] Jaffe, R.L., *Phys. Rev. D*, **15** (1977) 267
[2] LHCb collaboration, *JINST*, **8** (2013) P08002
[3] Belle collaboration, *Phys. Rev. Lett.*, **91** (2003) 262001
[4] D0 collaboration, *Phys. Rev. Lett.*, **93** (2004) 162002
[5] CDF collaboration, *Phys. Rev. Lett.*, **103** (2009) 152001
[6] BaBar collaboration, *Phys. Rev.*, **D82** (2010) 011101
[7] LHCb collaboration, *Eur. Phys. J.*, **C72** (2012) 1972
[8] CMS collaboration, *JHEP*, **04** (2013) 154
[9] BESIII collaboration, *Phys. Rev. Lett.*, **112** (2014) 092001
[10] Belle collaboration, *Lepton Photon conference proceedings*, **arXiv** (2005) 0505037
[11] Swanson, E., *Phys. Lett.*, **B598** (2004) 197
[12] Maini, L., Piccinini, F., Polosa, A.D., Riquer, V., *Phys. Rev.*, **D71** (2005) 014028
[13] Li, Bing An, *Phys. Lett.*, **B605** (2005) 306
[14] Seth, Kamal K., *Phys. Lett.*, **B612** (2005) 1
[15] Matheus, R.D., Navarra, F.S., Nielsen, M., Zanetti, C.M., *Phys. Rev.*, **D80** (2009) 056002
[16] CDF collaboration, *Phys. Rev. Lett.*, **98** (2007) 132002
[17] LHCb collaboration, *Phys. Rev. Lett.*, **110** (2013) 222001
[18] LHCb collaboration, *Phys. Rev.*, **D92** (2015) 011102
[19] BaBar collaboration, *Phys. Rev.*, **D74** (2006) 071101
[20] Li, Bai-Qing and Chao, Kuang-Ta, *Phys. Rev.*, **D79** (2009) 094004
[21] Ferretti, J., Galatà, G. and Santopinto, E., *Phys. Rev.*, **D90** (2014) 054010
[22] Badalian, A. M., Orlovsky, V. D., Simonov, Yu.A., and Bakker, B. L. G., *Phys. Rev.*, **D85** (2012) 114002
[23] BaBar collaboration, *Phys. Rev. Lett.*, **102** (2009) 132001
[24] Belle collaboration, *Phys. Rev. Lett.*, **107** (2011) 091803
[25] LHCb collaboration, *Nucl. Phys.*, **B886** (2014) 665
[26] Belle collaboration, *Phys. Rev. Lett.*, **100** (2008) 142001
[27] Rosner, J. L., *Phys. Rev.*, **D76** (2007) 114002
[28] Liu, Y-R., and Zhang, Z-Y., *arXiv*, **2009** (0908.1734)
[29] Maiani, L., Polosa, A. D., and Riquer, V., *New J. Phys.*, **10** (2008) 073004
[30] LHCb collaboration, *Phys. Rev. Lett.*, **112** (2014) 222002
[31] CLEO collaboration, *Phys. Rev.*, **D63** (2001) 092001
[32] LHCb collaboration, *Phys. Rev. Lett.*, **111** (2013) 102003
[33] LHCb collaboration, *Phys. Rev. Lett.*, **115** (2015) 072001